Development 127, 3215-3226 (2000)
Printed in Great Britain © The Company of Biologists Limited 2000
DEV4373

MesP1 and MesP2 are essential for the development of cardiac mesoderm

Satoshi Kitajima, Atsuya Takagi, Tohru Inoue and Yumiko Saga*

Cellular and Molecular Toxicology Division, National Institute of Health Sciences, 1-18-1 Kamiyohga, Setagaya-ku, Tokyo 158-8501, Japan

*Author for correspondence (e-mail: saga@nihs.go.jp)

Accepted 9 May; published on WWW 10 July 2000

Summary

The transcription factors, MesP1 and MesP2, sharing an almost identical bHLH motif, have an overlapping expression pattern during gastrulation and somitogenesis. Inactivation of the *Mesp1* gene results in abnormal heart morphogenesis due to defective migration of heart precursor cells, but somitogenesis is not disrupted because of normal expression of the *Mesp2* gene. To understand the cooperative functions of MesP1 and MesP2, either a deletion or sequential gene targeting strategy was employed to inactivate both genes. The double-knockout (dKO) embryos died around 9.5 days postcoitum (dpc) without developing any posterior structures such as heart, somites or gut. The major defect in this double-knockout embryo was the apparent lack of any mesodermal layer between the endoderm and ectoderm. The abnormal accumulation of cells in the primitive streak indicates a defect in the migratory activity of mesodermal cells. Molecular markers employed to characterize the phenotype revealed a lack of the cranio-cardiac and paraxial mesoderm. However, the axial mesoderm, as indicated by brachyury (*T*) expression, was initially generated but anterior extension was halted after 8.5 dpc. Interestingly, a headfold-like structure developed with right anterior-posterior polarity; however, the embryos lacked any posterior neural properties. The persistent and widely distributed expression of *Cerberus-like-1(Cer1)*, *Lim1* and *Otx2* in the anterior endoderm might be responsible for the maintenance of anterior neural marker expression. We also performed a chimera analysis to further study the functions of MesP1 and MesP2 in the development of mesodermal derivatives. In the chimeric embryos, dKO cells were scarcely observed in the anterior-cephalic and heart mesoderm, but they did contribute to the formation of the somites, notochord and gut. These results strongly indicate that the defect in the cranial-cardiac mesoderm is cell-autonomous, whereas the defect in the paraxial mesoderm is a non-cell-autonomous secondary consequence.

Key words: MesP1, MesP2, Gastrulation, Mesoderm, Heart morphogenesis, Neural patterning, Chimera analysis, Somite

INTRODUCTION

The process of gastrulation is a pivotal step in the formation of the vertebrate body plan. The primary function of gastrulation is the correct placement of precursor tissues for subsequent morphogenesis. In the mouse, gastrulation begins at 6.5 dpc with the delamination of epiblast cells into the primitive streak at the posterior limit of the embryo (for a review, see Tam and Behringer, 1997). Although cells may not be irrevocably committed to specific fates in different regions of the streak epiblast, there is a predictable regional establishment of specific cell populations within the gastrulating embryo. The most posterior region of the primitive streak predominantly gives rise to the extraembryonic mesoderm, which lines the yolk sac and produces embryonic blood cells. In contrast, the mid- and anterior streaks, at the late egg-cylinder stages, exclusively form the embryonic mesoderm. The mid-streak gives rise to the ventral (lateral) mesoderm that lines body cavities and generates mesodermal derivatives such as the kidney, whereas the anterior streak forms the paraxial somitic mesoderm. The definitive endoderm and dorsal midline of the notochord and head process are formed at the most extreme anterior end of the streak from the node region. The heart is one of the first structures that are formed during organogenesis in the mouse embryo (DeRuiter et al., 1992). Previous fate-mapping studies have identified the lateral epiblast as the major source of the embryonic mesoderm, including the heart mesoderm, which is localized in the posterior regions of the lateral epiblast (Lawson et al., 1991; Lawson and Pedersen, 1992; Parameswaran and Tam, 1995), and is colocalized with the cranial mesenchyme in the distal region of the newly formed mesodermal layer of the mid-primitive-streak-stage embryo (Tam et al., 1997). Therefore, mesodermal cell layers are generated in a sequential order, consisting first of the extraembryonic layer, followed by the cranial and cardiac, lateral, paraxial and axial embryonic layers. There are many reports of mesodermal deficiency, which include those in naturally occurring mutants such as msd (Holdener et al., 1994) and eed (Faust et al., 1998), and in several gene-knockout mice such as *cripto* (*Tdgf1*) (Ding et al., 1998), *Nodal* (Conlon et al., 1994), *Fgfr1* (Yamaguchi et al., 1994), *Fgf8* (Sun et al., 1999) and *Smad2* (*Madh2)* (Waldrip et

al., 1998). However, there has been no report of any mutation associated with the lack of cranial-cardiac mesoderm with intact somitic and/or axial mesodermal lineages. This may suggest that there is some dependence of the development of later mesodermal lineages on the generation of the earlier ones.

MesP1 and MesP2 are transcription factors containing an almost identical bHLH motif. They are encoded by the *Mesp1* and *Mesp2* genes, respectively, both located on chromosome 7, and separated by only 16 kb in the mouse (Saga et al., 1996, 1997). *Mesp1* is expressed in the early mesoderm that is destined to become the extraembryonic and cranial-cardiac mesoderm. An actual lineage study revealed that *Mesp1* is the earliest molecular marker expressed in the heart precursor cells (Saga et al., 1999). Previously, we generated MesP1- and MesP2-single-knockout mice to define their respective functions. Disruption of the *Mesp1* gene resulted in a morphogenetic abnormality of the heart, cardia bifida (Saga, 1998). Analyses of *Mesp2*-single-knockout mice revealed the critical requirement of MesP2 for the normal segmentation of somites, generation of the rostral identity of the sclerotome and maintenance of the rostrocaudal polarity of somites (Saga et al., 1997). No notable defect was observed before somitogenesis in *Mesp2*-deficient mice, however, which was consistent with the apparent lack of expression of *Mesp2* during the early gastrulation stage. Analyses of *Mesp1*$^{-/-}$ embryos revealed that the defect is due to the delayed migratory activity of mesodermal cells; however, an abnormal heart was eventually generated in association with mesodermal migration (Saga et al., 1999). We expect that this might be the result of upregulation of the *Mesp2* gene. Thus, we examined *Mesp2* expression in *Mesp1*$^{-/-}$ embryos and detected *Mesp2* expression in *Mesp1*$^{-/-}$ embryos. Armed with the knowledge that these genes are able to function redundantly during somitogenesis, we were prompted to generate double-knockout (dKO) mice to define the precise functions of these two genes during gastrulation. We employed two alternative strategies, deletion and sequential targeting, to generate double-knockout mice. These strategies generated mice with a basically identical phenotype. Embryos deficient in both MesP1 and MesP2 lacked most of embryonic nonaxial mesoderm, and no posterior trunk structures developed. Furthermore, a chimera analysis revealed that the defect in the generation of the cranial and cardiac mesoderm in *Mesp1*$^{-/-}$, *Mesp2*$^{-/-}$ cells was cell-autonomous, but that this was not the case for the generation of paraxial mesoderm.

MATERIALS AND METHODS

Vector construction and homologous recombination

Genomic clones for mouse *Mesp1* and *Mesp2* were isolated by screening a genomic library established in λ FixII from TT2 ES cell DNA with a *Mesp1* cDNA probe (Saga, 1998). To delete a genomic region of approximately 20 kb containing the entire coding exons of *Mesp1* and *Mesp2*, a 6.5-kb DNA fragment located about 4 kb downstream of the *Mesp1* gene and a 1-kb fragment located about 2 kb downstream of the *Mesp2* gene were used as the long and short homology arms for the targeting vector (TV-Del) (Fig. 1). For sequential targeting, ES clone #96, originally obtained to generate *Mesp1*$^{-/-}$ mice (Saga, 1998), was used to integrate a second homologous recombination on the *Mesp2* locus. The targeting vector (TV-P2-cre) was constructed to knock-in Cre-recombinase in-frame, so that the long homology arm started from just upstream of the translational initiation site for the *Mesp2* gene and spanned 6 kb upstream. For the short arm, the same DNA fragment as that employed to construct TV-Del was used. For positive selection, *pgk-puromycin* (Watanabe et al., 1995) was used instead of *pgk-neomycin*. These vectors were linearized at the *Not*I site and introduced into TT2 ES cells [C57BL/6(B6)/CBA] or *Mesp1*$^{+/-}$ #96 cells by electroporation as described previously (Yagi et al., 1993). After selection using either G418 or puromycin, the resistant clones were isolated and their DNAs were analyzed by PCR using a primer PGK-R (for P2-cre) or NeoAL2 (for Del), and a *Mesp2* genomic primer P2-GR3. The sequences for these primers were: PGK-R: 5′-CTAAAGCGCATGCTCCAGACT-3′, NeoAL2: 5′-GGGGATGCGGTGGGCTCTATGGCTT-3′ and MesP2-GR3:5′-GGAAGTTGAGTTCCTCATCACGATC-3′, respectively.

Generation of chimeric mice

Embryo manipulations and injection of the ES cell clones into ICR 8-cell embryos were carried out as described previously (Yagi et al., 1993). Alternatively, ES cells were aggregated (5-10 cell clumps) with 8-cell embryos treated with Tyrode's solution and incubated for 24 hours to obtain blastocysts. Chimeric mice with a high contribution of the TT2 genetic background (monitored by the agouti coat color) were bred with ICR mice.

Generation of chimeric embryos

Chimeric embryos were generated by aggregating 8-cell embryos of the wild-type (ICR) with those of the mutant mice, which were genetically marked with the ROSA26 transgene (+/–) (Zambrowicz et al., 1997). Mutant embryos were generated by crossing *Mesp1, p2*-del$^{+/-}$ mice, generated using the targeting vector TV-Del, and *Mesp1, p2*-null$^{+/-}$ mice generated by TV-P2-cre, to distinguish chimeric embryos derived from homozygous embryos that have a mutated allele both for *Mesp1, p2*-del and *Mesp1, p2*-null, from heterozygous embryos derived from either *Mesp1, p2*-del$^{+/-}$ or *Mesp1, p2*-null$^{+/-}$ mice. Therefore, only 3/16 chimeric embryos were expected to be chimeric with mutant embryos marked with ROSA. The genotype of the chimeric embryos was determined by PCR using yolk-sac DNA.

Embryo analysis by β-gal staining, whole-mount in situ hybridization and sectioning of samples

The fixed chimeric embryos at various developmental stages were stained for the detection of β-galactosidase activity, as described previously (Saga et al., 1992). The basic method used for whole-mount in situ hybridization has also been described previously (Saga et al., 1996), although no glycine treatment was performed after the Proteinase K treatment. For preparing sections, samples stained by β-gal or for in situ hybridization were postfixed with 4% paraformaldehyde and embedded in paraffin wax or plastic resin (technovit 8100, Heraeus Kulzer, Inc.) after dehydration in a graded ethanol series.

RESULTS

Mesp1$^{-/-}$ embryo exhibits expression of *Mesp2* that may compensate for the deficiency of MesP1 function during gastrulation

The abnormal heart morphogenesis in *Mesp1*$^{-/-}$ embryos resulting in cardia bifida is caused by delayed migration of the heart precursor cells (Saga et al., 1999); however, the initial suppression of cell migration appeared to be rescued during the later stages of development. The mesodermal cells gradually migrated out from the primitive streak and moved toward the heart field. Therefore, we expect that *Mesp2*, another gene of the same family, might be activated and serve the function of

MesP1. Indeed, our knock-in study revealed that MesP2 has the ability to substitute for MesP1 function during heart morphogenesis (our unpublished data). Therefore, we analyzed whether *Mesp2* was activated in the absence of MesP1 in the early- to late-gastrulation-stage embryos. As clearly shown in Fig. 2A-C, *Mesp1* is expressed strongly in the early gastrulating embryo (6.5-6.75 dpc), but its expression was rapidly downregulated after 7.5 dpc. In contrast, we had never previously detected *Mesp2* expression at 6.5-7.5 dpc. Prolonged in situ reaction, however, revealed *Mesp2* expression at 6.5-7.0 dpc in both wild-type and *Mesp1*$^{-/-}$ embryos (Fig. 2D), in a pattern very similar to that of *Mesp1*. Interestingly, *Mesp2* expression in *Mesp1*$^{-/-}$ embryos was retained for longer than that in wild-type embryos and it was easily detected at 7.5 dpc (Fig. 2E), whereas wild-type embryos of the same litter did not show any significant expression of *Mesp2*. Therefore we concluded that *Mesp2* is expressed during the gastrulation stage, just like *Mesp1*, but

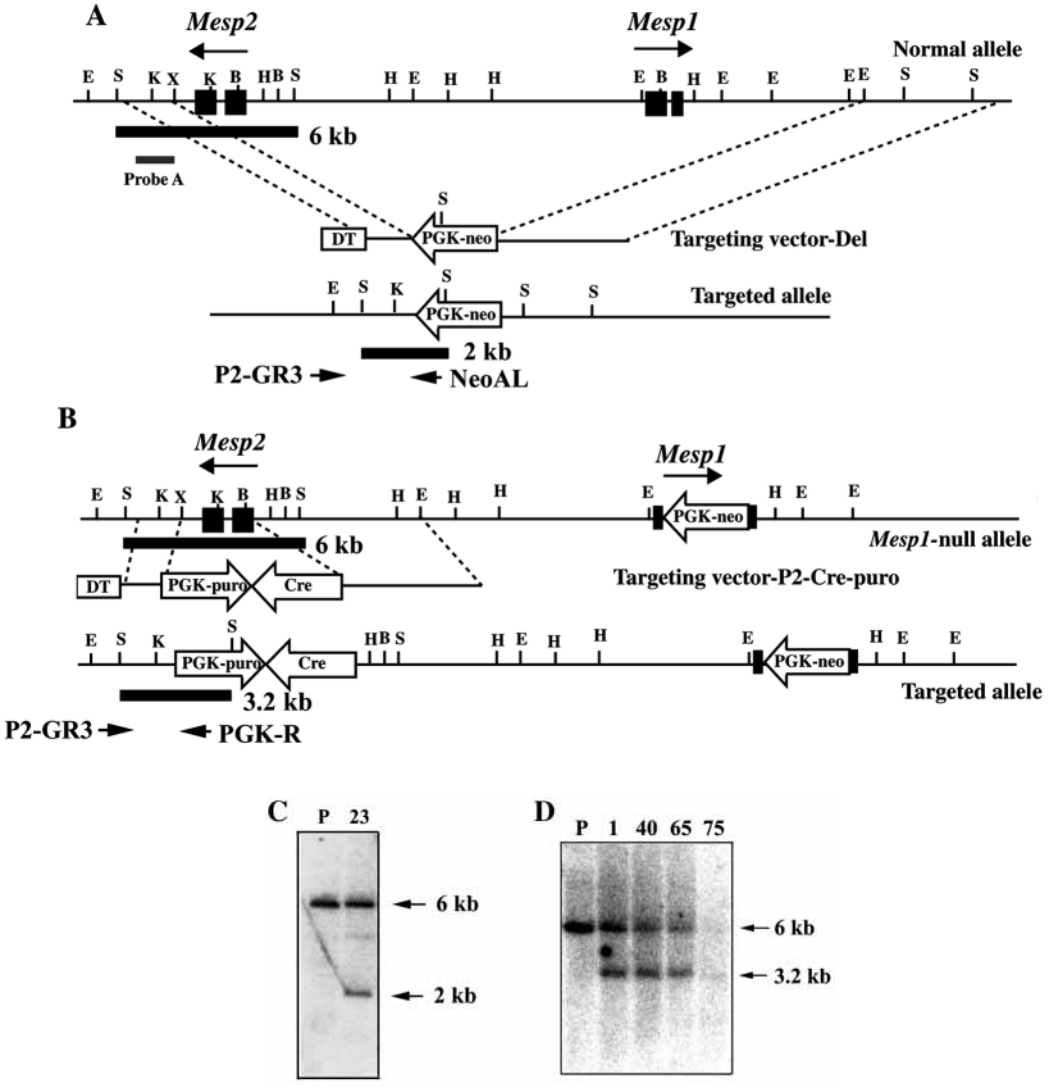

Fig. 1. Generation of double-knockout (dKO) mice by either deletion (A,C) or sequential gene targeting (B,D). (A) Schematic representation of the targeting strategy by deletion. A genomic DNA region of approximately 20 kb containing both *Mesp1* and *Mesp2* coding sequences was replaced with the *pgk-neo* cassette by a single homologous recombination. A genomic fragment downstream of the *Mesp1* gene (about 7 kb) and a 1-kb fragment located downstream of the *Mesp2* gene served as the long and short homology arms, respectively. The black boxes represent either *Mesp1* or *Mesp2* exons. Arrows indicate the primers used for the PCR. The large open arrow represents the orientation of the *pgk-neo* cassette. Probe A was used for the Southern blot analysis to distinguish mutant alleles from normal alleles. DT, diphtheria toxin fragment-A. B, *Bam*HI; E, *Eco*RI; H, *Hin*dIII; K, *Kpn*I; S, *Sac*I; X, *Xba*I. (B) Schematic representation of the targeting strategy for *Mesp2-Cre*. A targeting vector was designed to replace the Cre recombinase coding sequence with *Mesp2* coding exons. The targeting vector was introduced into the ES cell clone #96, which had been disrupted previously at the *Mesp1* locus by *pgk-neo* replacement (Saga, 1998). The large open arrows show the orientation of *pgk-puro*, Cre recombinase, and the *pgk-neo* cassette. (C) Genomic Southern blot analysis of PCR-positive ES cell DNA obtained using the targeting vector, TV-Del. P, parental TT2 ES cells. Arrows indicate the 2-kb *Sac*I fragment of the mutant allele and the wild-type 6-kb fragment. (D) Genomic Southern blot analysis of PCR-positive clones obtained with the targeting vector, P2-Cre-puro. Probe A, shown in A, was also used here. Arrows indicate the 3.2-kb *Sac*I fragment of the mutant allele and the wild-type 6-kb fragment.

this expression is only detected with difficulty because it occurs at low levels and is transient. Since MesP2 must thus also be functioning during gastrulation, the possibility was suggested that the prolonged *Mesp2* expression observed in *Mesp1*$^{-/-}$ embryos might rescue the phenotype. Therefore, we attempted to generate *Mesp1*- and *Mesp2*-double-knockout mice to clarify the function of MesP2 during gastrulation and to understand the cooperative functions of the two transcription factors. However, with these genes being located next to each other on the same chromosome, we did not attempt to generate double-knockout mice by crossing two single-knockout mice, and instead we employed the following two alternative strategies, deletion and sequential targeting.

Targeting strategies to generate *Mesp1*$^{-/-}$, *Mesp2*$^{-/-}$ double-knockout mice

For the deletion strategy, a targeting vector was designed to remove a large genomic region that included both *Mesp1* and *Mesp2* genes (Fig. 1A). The linearized vector was introduced into TT2 ES cells by electroporation and G418-resistant cells were subjected to screening by PCR. One PCR-positive clone (#23) was further analyzed by Southern hybridization analysis to confirm it as being a correct homologous recombinant (Fig. 1C). The ES cells were injected into 8-cell embryos and chimeric mice were generated. The chimeras were successfully transferred to the next generation and we established a dKO mutant mouse line (we refer to this line as *Mesp1, p2*-del). As an alternative strategy, a previously obtained heterozygous *Mesp1*$^{+/-}$ ES cell clone #96 (Saga, 1998) was subjected to a second round of electroporation using a targeting vector designed for *Mesp2* disruption with the *puromycin* gene as the positive selection marker (Fig. 1B). Four positive clones detected by both PCR and Southern blot analysis (Fig. 1D) were further analyzed by FISH to confirm whether the second targeting event was integrated in the same chromosome as the one in which the *Mesp1* gene was disrupted. Fortunately, all of the four clones were identified to have the desired configuration (data not shown). Two clones were used for chimera production, of which one gave rise to a germline chimera (we refer to this mouse line as *Mesp1, p2*-null). Once the *Mesp1, p2*-del line was established, however, we were not confident that the phenotype observed (described below) was solely a consequence of the lack of only the *Mesp1* and *Mesp2* genes, since there could have been other gene(s) in the deleted region. Embryos of the *Mesp1, p2*-null line generated by sequential targeting were similar in terms of both the morphology and marker gene expression to the *Mesp1, p2*-del embryos (data not shown). Thus, we concluded that the phenotype of *Mesp1, p2*-del is indeed due only to the lack of the *Mesp1* and *Mesp2* genes. Therefore, most of the results shown in this paper are those obtained by the analysis of *Mesp1, p2*-del mice, unless otherwise stated.

Mesodermal defects in the *Mesp1, p2*-del embryo

The heterozygous mice showed no differences from the wild-type mice. Since we already knew that *Mesp1*$^{-/-}$ mice began to show abnormalities from 7.5 dpc and died before 10.5 dpc, we analyzed intercrossed embryos from 7.5 dpc. As shown in Fig. 3A, *Mesp1, p2*-del embryos exhibited clear differences from their wild-type littermates at 7.5 dpc. They were smaller in size, especially in the anterior region, while thickening of the posterior primitive streak region was noted. Examination of cross sections confirmed the initial observations. *Mesp1, p2*-del embryos exhibited abnormal gastrulation, with no clear mesodermal cell layer between the endoderm and the ectoderm. Dense cell accumulation in the primitive streak, however, indicated the initiation of gastrulation and the ingression of ectodermal cells into the primitive streak, but the mesodermal cells appeared unable to depart from the primitive streak. Similarly, in the extraembryonic region, many mesodermal cells were accumulated at the proximal junction between the embryonic and extraembryonic region, but cells in the extraembryonic region were not as tightly packed as those in the primitive streak. In *Mesp1, p2*-del embryos at 8.5 dpc, we noticed a sign of headfold curvature; however, no distinct head protrusion was observed (Fig. 3B). The cross sections revealed similar morphology to that of 7.5-dpc embryos; no clear mesodermal cell layer, but a thickening of the cell layer was observed in both the ectoderm and the primitive streak. At 9.0-9.5 dpc, an extensive pile-up of cell layers in the extraembryonic region was seen in the mutant embryos (Fig.

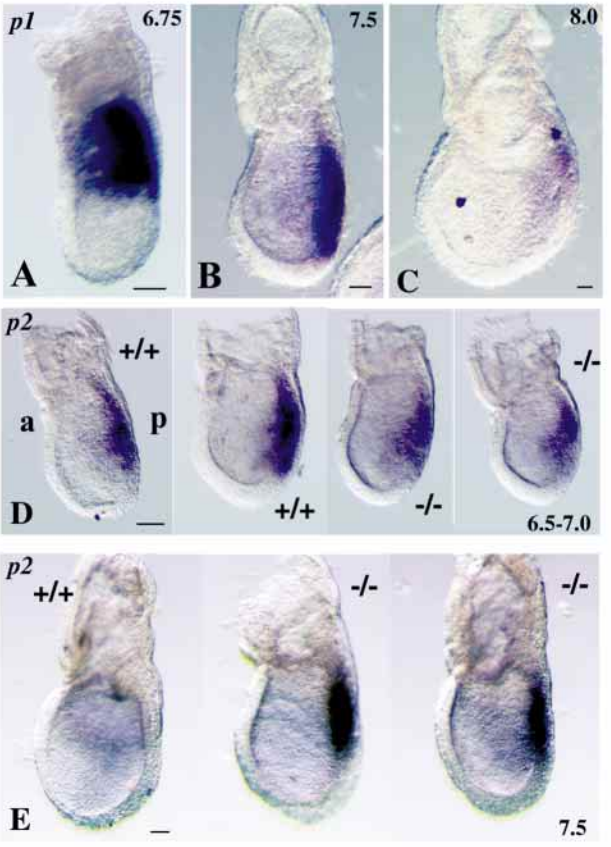

Fig. 2. *Mesp1* or *Mesp2* expression in *Mesp1*$^{-/-}$ and wild-type embryos. *Mesp1* is strongly expressed during gastrulation (A,B) but downregulated after 7.5 dpc (C). *Mesp2* expression is detected in the wild-type embryo at 6.5-7.0 dpc, but is downregulated before 7.5 dpc (+/+ in D,E), while more prolonged *Mesp2* expression than in wild-type littermates is observed in *Mesp1*$^{-/-}$ embryos (–/– in D,E). (A-C) Color development was conducted for 4 hours at room temperature (RT); (D,E) the samples were subjected to prolonged reaction (an additional 12 hours at 4°C after 4 hours at RT). The embryonic stages (dpc) are indicated in each figure. *p1*, *Mesp1* probe; *p2*, *Mesp2* probe. Bars, 100 μm.

3C1,3). In contrast, the embryonic region was smaller and showed numerous abnormalities. The headfold-like structure (arrows, Fig. 3C1) had developed, but no trunk structure such as the heart, somites or gut was observed. Examination of the cross sections of the extraembryonic region (Fig. 3C2-4) revealed numerous mesodermal-like cells in the distal part of the extraembryonic region (Fig. 3C3). Furthermore, the development of endothelial cells indicated the initiation of vasculogenesis although no distinct blood vessels were observed (Fig. 3C3,4). An allantois-like structure was also observed in the *Mesp1, p2*-del embryo (Fig. 3C2). In contrast, no clear mesodermal layer was recognized in the embryonic region. Extensive cell debris (arrows, Fig. 3C3) was observed in the amniotic cavity in the *Mesp1, p2*-del embryo after 9.0 dpc. These observations suggest that the ingressed mesodermal cells either migrated into the extraembryonic region or died in the embryonic region.

Because morphological and histological analyses of *Mesp1, p2*-del embryos demonstrated striking defects in the formation of the embryonic mesoderm, we further analyzed these defects by examining the expression of appropriate marker genes for specific tissues in embryos dissected at 7.5-8.5 dpc.

Genetic activities in the primitive streak

Because either *Mesp1* or *Mesp2* is expressed in the nascent mesoderm, we expected that the primitive streak would be generated normally; however, the genetic activities in the primitive streak could be affected by the defect in the mesoderm. *Brachyury* (*T*) is a good marker for both the primitive streak and the axial mesoderm (Herrmann et al., 1990). We observed strong expression in the primitive streak of a 7.5-dpc *Mesp1, p2*-del embryo, similar to that in the wild-type embryo (Fig. 4A). *Fgf4*, *Fgf8* and *Nodal* are implicated as

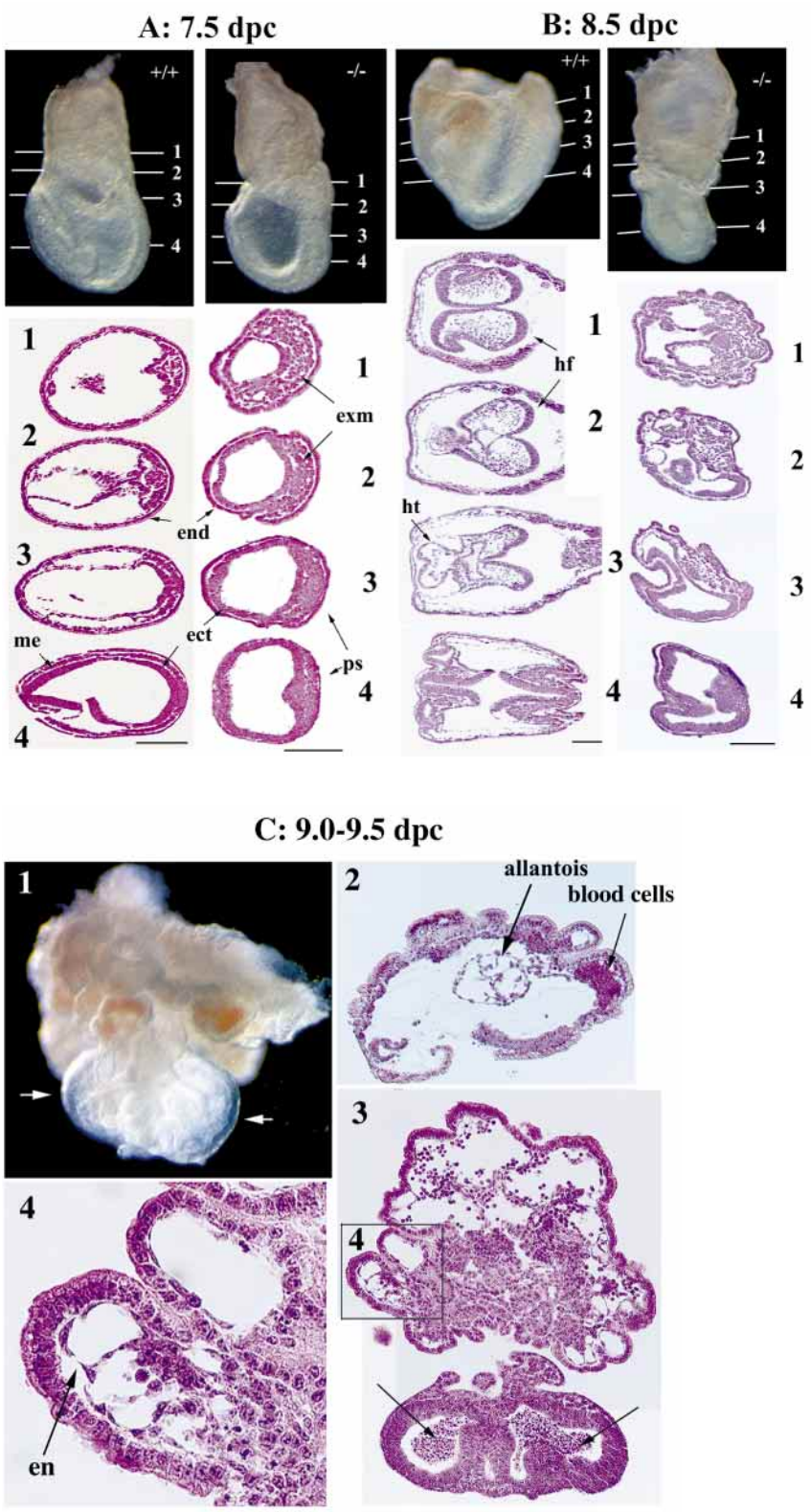

Fig. 3. The *Mesp1, p2*-del embryo shows defective development of the mesoderm. (A) lateral view of the wild-type embryo and *Mesp1, p2*-del embryo at 7.5 dpc. Cross sections of the *Mesp1, p2*-del embryo reveal abnormal gastrulation with accumulation of mesodermal cells in the posterior region. No mesodermal layer is present between endodermal and ectodermal layers. Similarly, at 8.5 dpc, although the wild-type embryo shows development of the heart tube and mesenchymal cells in the headfold (B), the *Mesp1, p2*-del embryo still does not show migration of mesodermal cells. At 9.0-9.5 dpc (C), the *Mesp1, p2*-del embryo shows an extensive pile-up of mesodermal cells in the extraembryonic region and only a headfold-like structure (arrows in C1) is observed in the embryonic region. Cross sections reveal extensive blood island formation in the extraembryonic region (C2). Cell death is prominent in the embryonic region (arrows, C3). The presence of differentiated endothelial cells and tubular formation indicate vasculogenetic activities (C4). ect, ectoderm; end, endoderm; en, endothelial cells; exm, extraembryonic mesoderm; me, embryonic mesoderm; hf, headfold; ht, heart; ps, primitive streak. Bars, 100 μm.

signaling molecules for the formation of the primitive streak and the mesoderm. They are expressed in the cells within the primitive streak and are downregulated shortly after they exit it (Crossley and Martin, 1995; Sun et al., 1999; Zhou et al., 1993). *Fgf8* and *Nodal* were expressed in the *Mesp1, p2*-del embryo (Fig. 4D-F,I-L) and were retained for longer than those in the wild-type embryo, especially in the case of *Nodal* (Fig. 4I,J). Interestingly, however, *Fgf4* expression was not observed in the *Mesp1, p2*-del embryo (Fig. 4K,L). *Evx1*, a homeobox gene that is also implicated in normal primitive streak formation (Faust et al., 1995), was expressed in the *Mesp1, p2*-del embryo but the expression was localized in the proximal region and did not extend to the distal end as observed in wild-type embryo (Fig. 4M,N). We also examined the organizer activities of primitive streak by analyzing *goosecoid* (*Gsc*) expression (Blum et al., 1992). In the wild-type embryo at 6.5-7.0 dpc, *Gsc* is expressed at the anterior end of the primitive streak and later, it is expressed in the prechordal plate (Fig. 4G). In the *Mesp1, p2*-del embryo, rather stronger *Gsc* expression was observed in the expanded region in the primitive streak even at the later stage (Fig. 4H). Therefore, the initial formation of primitive streak occurs normally even in the *Mesp1, p2*-del embryo; however, the genetic activity in the primitive streak might be modulated by the defect in the mesoderm. Next, we analyzed whether mesodermal ingression occurs normally and whether or not the ingressed cells show any mesodermal characteristics.

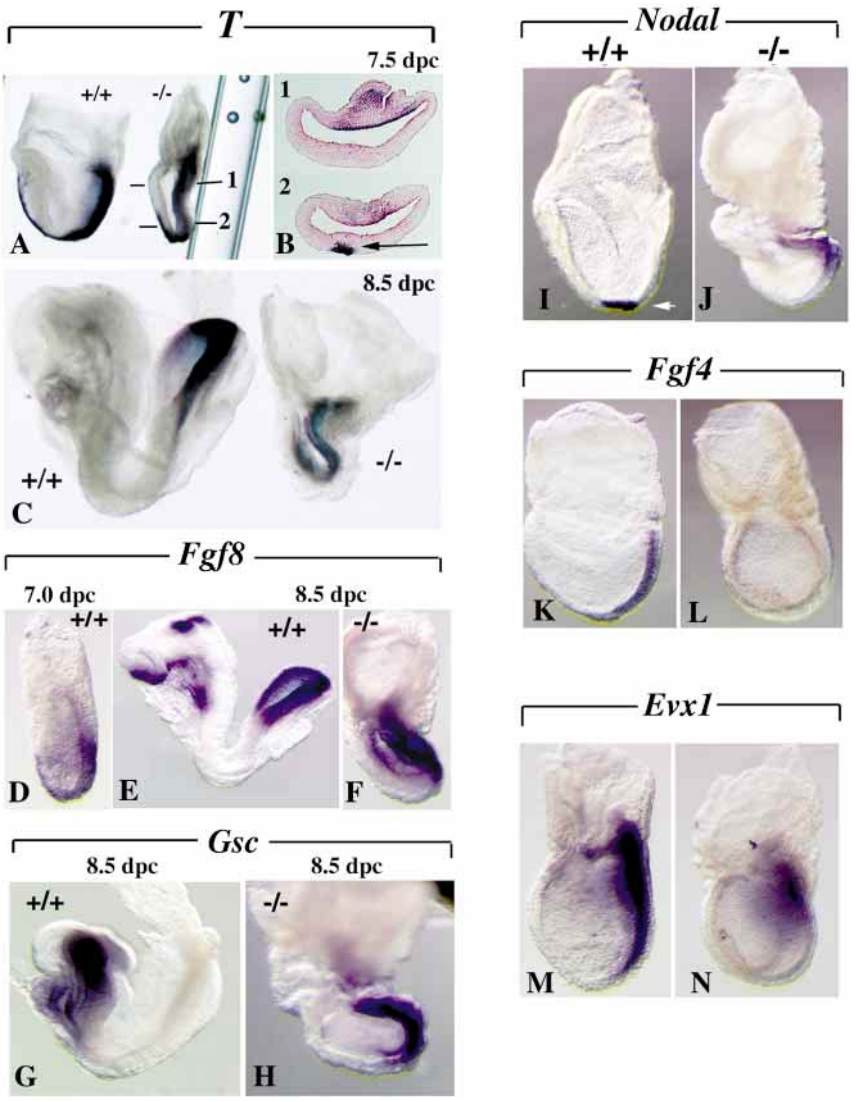

Fig. 4. Gene expression in the primitive streak. *T* expression demarcating the primitive streak and the axial mesoderm is normally observed even in the *Mesp1, p2*-del embryo at 7.5 dpc (A), but no more rostral elongation was observed after 8.5 dpc (C). Transverse sections of a *Mesp1, p2*-del embryo at 7.5 dpc reveal anteriorly extended *T* expression, indicating the existence of axial mesodermal cells (B, arrow). Strong expression in the primitive streak was retained for *Fgf8* (D-F), *goosecoid* (*Gsc*) (G,H) and *Evx1* (M,N). Normally *Nodal* expression in the primitive streak is quickly downregulated and localized in the node (arrow, I), while its expression is retained in the primitive streak in the *Mesp1, p2*-del embryo (J). *Fgf4* expression observed in wild-type embryo (K) is not detected in the *Mesp1, p2*-del embryo (L). Developmental stages are indicated in A-H. Embryonic stages I-N are between 7.5-8.0 dpc.

Mesp1, p2-del embryos may lack embryonic non-axial mesoderm

Most known mesodermal markers are also expressed in other regions such as the primitive streak or the endoderm. The most specific mesodermal marker available so far, except for *Mesp1* or *Mesp2*, is *Lefty2*, which is expressed in the nascent mesoderm in a pattern very similar to that of *Mesp1* (Meno et al., 1999). Interestingly, *Lefty2* is not detected in the *Mesp1, p2*-del embryo even at 7.5 or 8.5 dpc (Fig. 5A,B). *Lim1* is known to be expressed in the anterior and posterior endoderm in addition to the mesoderm, but its expression in the nascent mesodermal wing is very similar to that of *Mesp1* (Fig. 5C,D; Perea-Gomez et al., 1999). *Lim1* expression in the *Mesp1, p2*-del embryo was observed in the posterior region, similar to the case in the wild-type embryo (Fig. 5E). Serial sections were prepared to determine the cell types expressing *Lim1*. As shown in Fig. 5F, the outermost endodermal cells lacked the signal and the *Lim1* signal was observed in the thin layer underlying the negative outer cells, although most of the mesodermal-like posterior cell mass was negative for the signal. The result therefore indicates that the *Mesp1, p2*-del embryo generates at least *Lim1*-positive mesodermal cells and *Lim1* is in the upstream of MesP1 or in a different cascade. As expected by the lack of further mesodermal migration, the cardiac mesodermal marker, *Nkx2-5* (Biben and Harvey, 1997), and an early marker for cranial mesoderm, *Tbx1* (Chapman et al., 1996), were not detected in the mesodermal-like cells (data not shown). Furthermore, paraxial mesoderm, which ingresses through the primitive streak after the cranial and cardiac mesoderms, was not detected at all when examined by *Mox1* expression (Fig. 5G,H; Candia et al., 1992). Therefore, among the cells that

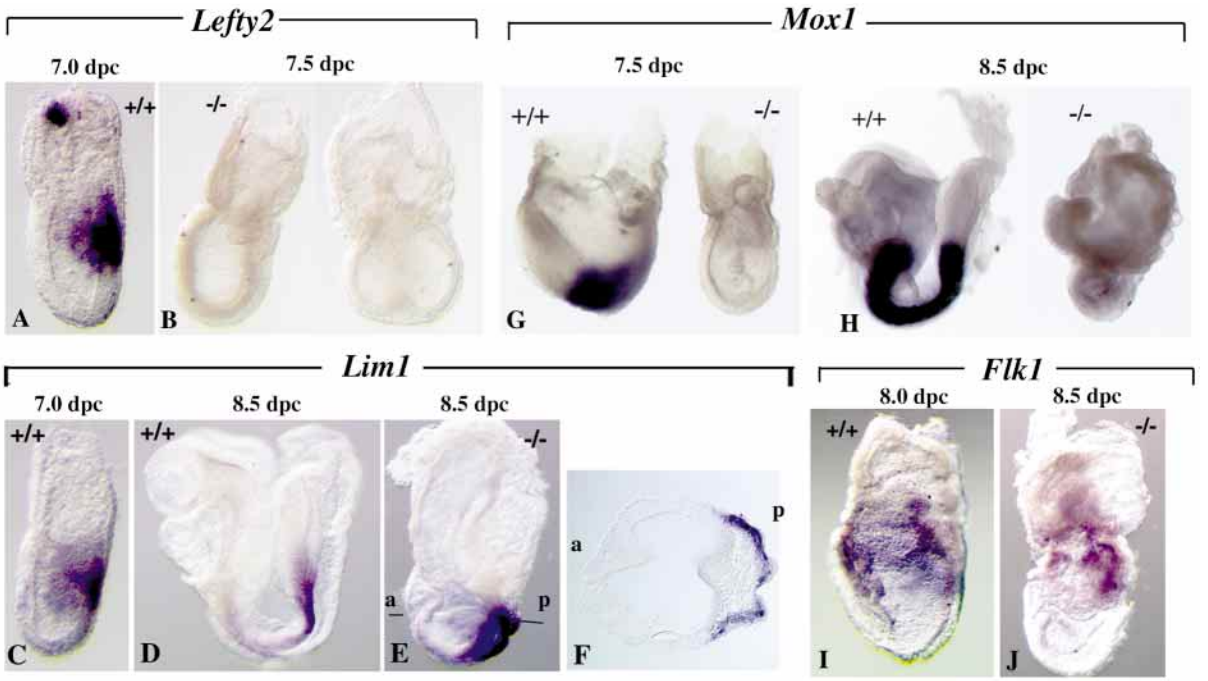

Fig. 5. Gene expression of mesodermal markers. Early expression of *Lefty2* is restricted to newly formed mesoderm (A). In the *Mesp1, p2*-del embryo, no *Lefty2* expression is observed (B; lateral view to the left and posterior view to the right). The early expression domain of *Lim1* includes nascent mesodermal cells (C) and later the node region (D) in the wild-type embryo, while in the *Mesp1, p2*-del embryo, the expression was observed in the posterior region (E). Examination of a transverse section revealed that strong *Lim1* expression was observed in a thin mesodermal layer inside the outermost enodermal cells (F). a, anterior; p, posterior. *Mox1*, a marker of paraxial mesoderm, was not detected at all (G,H). *Flk1* was expressed in the extraembryonic region of the *Mesp1, p2*-del embryo (I,J).

accumulated in the primitive streak, only the mesodermal-like cells exiting the streak showed expression of the nascent mesodermal marker *Lim1* but not the other mesodermal markers. In contrast in the extraembryonic mesoderm, *Flk1*, which is a marker of cells destined to become hematopoietic and endothelial cells (Shalaby et al., 1997), was expressed in the prospective blood island region, although the expression was stronger toward the posterior side in the *Mesp1, p2*-del embryo (Fig. 5I,J). Finally, we focused on the axial mesodermal markers. Because both *Mesp1* and *Mesp2* are not expressed in the axial mesoderm and strong *Gsc* expression is observed in the primitive streak of *Mesp1, p2*-del embryos, we expected to detect the axial mesodermal cell population. Actually, some *T*-positive axial cells were observed in the 7.5-dpc embryo (Fig. 4A,B); however, no rostral elongation was observed in later-stage (at 8.5 or 9.5 dpc) embryos (Fig. 4C and data not shown). Furthermore, another axial mesodermal marker, *sonic hedgehog* (*Shh*), was not detected at all (data not shown). Therefore, axial mesodermal cells may emerge initially but may not fully differentiate as a typical axial mesoderm in the *Mesp1, p2*-del embryo.

Embryonic ectoderm of *Mesp1, p2*-del embryos expresses only anterior neuronal markers

The embryonic ectoderm of a 9.5-dpc *Mesp1, p2*-del embryo was morphologically similar to the headfold-like structure. To confirm the initial impression, we employed several ectodermal markers demarcating early neuronal development. At first, we used the *Otx2* probe to examine the ectodermal properties. Normally *Otx2* is expressed throughout the ectoderm prior to gastrulation, whereas at the headfold stage, it is restricted to the anterior region (Matsuo et al., 1995). In the *Mesp1, p2*-del embryo, however, strong *Otx2* expression was observed in the entire embryo, indicating that the ectoderm retained its primitive ectodermal property or further developed to acquire anterior head identity (Fig. 6A). To distinguish between these, we employed *Six3* as the probe. *Six3* is one of the most anterior genes marking the head structure, which later develops into the ectoderm of the nasal cavity, olfactory placode and Rathke's pouch (Oliver et al., 1995). As clearly shown in Fig. 6B, strong *Six3* expression was detected in the anterior half of the *Mesp1, p2*-del embryo, indicating that the ectoderm in the *Mesp1, p2*-del embryo developed enough to acquire the anterior neuronal identity. Similarly, *Hex*, the expression of which is also confined to the anteriormost endoderm and the headfold structure (Fig. 6C; Thomas et al., 1998), was normal in the *Mesp1, p2*-del embryo (Fig. 6D). To further examine the neuronal patterning, we examined *Gbx2* expression, the activity of which is important to establish a boundary between the midbrain and the anterior hindbrain (Wassarman et al., 1997). In the wild-type embryo, *Gbx2* is expressed as early as 7.5 dpc in the posterior half of the neural ectoderm and the primitive streak region (Fig. 6E). In the neuroectoderm, its expression pattern is clearly different from that of *Otx2*. In the *Mesp1, p2*-del embryo, however, we could not detect any expression between 7.5-9.5 dpc (Fig. 6E and data not shown). As expected by the complete lack of *Gbx2* expression, we could also not detect the expression of *En2* or *krox20* (data not

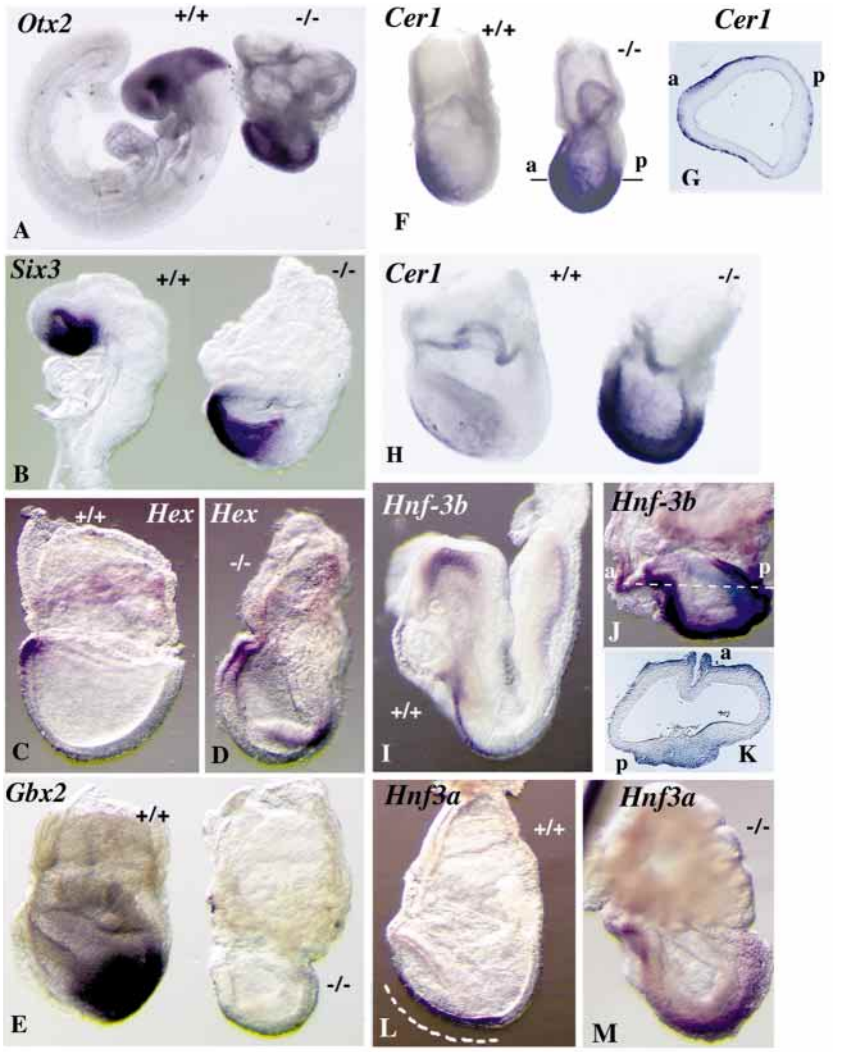

Fig. 6. Patterning of neuroectoderm and genetic activities underlyning the ectoderm. Anterior neural markers, *Otx2* (A), *Six3* (B) and *Hex* (C,D) were expressed even in the *Mesp1*, *p2*-del embryos. Expression of the posterior neural marker *Gbx2* (E), however, was absent in the *Mesp1*, *p2*-del embryo. *Cer1* (F-H) and *Hnf-3b* (I-K) were strongly expressed in the endoderm of *Mesp1*, *p2*-del embryos, as revealed in the transverse sections (G,K). a, anterior; p, posterior. *Hnf3a* was also observed in the *Mesp1*, *p2*-del embryo (M) but the expression was stronger in the posterior region, differing from the situation in the wild-type embryo (L). The expression domain in the wild type is indicated by a broken white line. Embryonic stages: A, 9.5 dpc; B,I-K, 8.5 dpc; C-E,H,L,M, 7.75-8.0 dpc; F,G, 7.5 dpc.

shown). Therefore, the headfold-like structure in the *Mesp1*, *p2*-del embryo is mostly composed of cells exhibiting anterior neural properties.

Next, we investigated the molecular mechanism underlying the maintenance of *Otx2* expression in the *Mesp1*, *p2*-del embryo. It has been shown that a positive signal from the anterior mesendoderm is required to stabilize the expression of *Otx2*, whereas a negative signal from the later-forming posterior mesendoderm repressed *Otx2* expression in the posterior part of the embryo (Ang et al., 1994). Although the molecular nature of these signals has not yet been defined, several genes expressed in the anterior mesendoderm, such as *cereberus-like 1* (*Cer1*), *Lim1* or *Nodal*, are implicated in the maintenance of preexisting anterior identity (Beddington and Robertson, 1999). We therefore examined the expression of these genes. Interestingly, strong *Cer1* expression was observed in the endoderm underlining the entire ectoderm in the 7.5 to 8.5-dpc *Mesp1*, *p2*-del embryo, whereas expression in the wild-type embryo was downregulated before 7.5 dpc (Fig. 6F-H). Furthermore in the endoderm, we observed strong expression of *Hnf-3b* (Fig. 6I-K), which was recently shown to work synergistically with *Lim1* to retain anterior ectodermal identity (Perea-Gomez et al., 1999). Therefore one of the mechanisms underlying the maintenance of *Otx2* expression is the persistent presence of endodermal signals to support anterior ectodermal identity. Lack of active migration of the definitive endoderm was also indicated by the expression pattern of *Gsc* (Fig. 4H) and *Hnf3a* (Fig. 6M; Sasaki and Hogan, 1993), which might also be a cause of the ectodermal abnormalities.

Cell-autonomous defect in the cardiac mesoderm

To clarify whether the mesodermal defect observed in the *Mesp1*, *p2*-del embryo is a cell-autonomous or non-cell-autonomous consequence, chimera analysis was conducted. Since we generated different alleles for the dKO phenotype, e.g. *Mesp1*, *p2*-del and *Mesp1*, *p2*-null, these heterozygous mice were bred to generate *Mesp1*$^{-/-}$, *Mesp2*$^{-/-}$ embryos, which were also marked by integration of the ROSA26 transgene (Zambrowicz et al., 1997). The 8-cell embryos obtained by intercrossing were aggregated with 8-cell embryos derived from the ICR mouse strain. Thus dKO/wild chimeric embryos, which can be identified by PCR, are composed of β-gal-negative wild-type cells and β-gal-positive *Mesp1*$^{-/-}$, *Mesp2*$^{-/-}$ cells. In total, we transferred 72 aggregates and recovered 36 embryos at either 8.5 or 9.5 dpc, of which five were aggregated with β-gal-positive *Mesp1*$^{-/-}$, *Mesp2*$^{-/-}$ cells. The result was extremely interesting. All the five embryos containing *Mesp1*$^{-/-}$, *Mesp2*$^{-/-}$ cells developed normally but the heart was composed only of wild-type cells and lacked *Mesp1*$^{-/-}$, *Mesp2*$^{-/-}$ cells (compare Fig. 7A-D and E-H). A clear difference was observed even in the 8.5-dpc embryo (Fig. 7A,E). Cross sections of these embryos confirmed the almost complete absence of *Mesp1*$^{-/-}$, *Mesp2*$^{-/-}$ cells in most of the heart tissue (compare Fig. 7J,K,N,O). Cells in the atrial appendage, however, were exclusively composed of *Mesp1*$^{-/-}$, *Mesp2*$^{-/-}$ cells, which may indicate a difference in cell lineage (Fig. 7O). In addition, the biased distribution of β-gal-positive cells was also observed in cross sections of the head mesenchyme (compare Fig. 7I,M,N) although whole-mount samples looked totally blue except for the heart. The contribution of wild-type cells was specifically observed only in the anterior head mesenchyme, whereas both cells contributed in the posterior region, indicating that *Mesp1* and *Mesp2* are required for the migration of the anteriormost

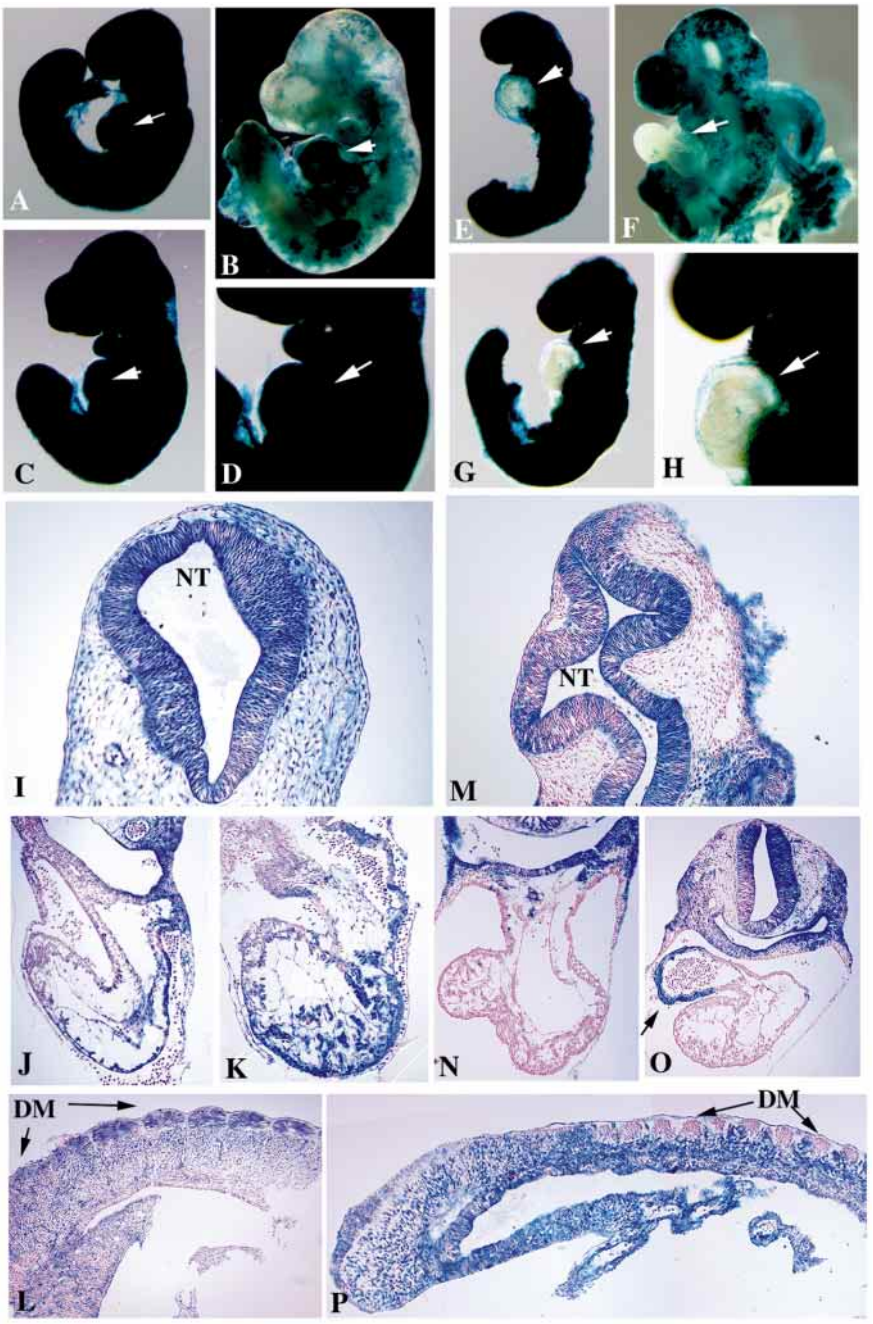

Fig. 7. Analyses of chimeric embryos generated by aggregating 8-cell embryos of dKO(Rosa) or wild(Rosa) with the wild-type embryo. (A-D,I-L) Chimeras of wild (Rosa)/wild type. (E-H,M-Q) Chimeras of the dKO(Rosa)/wild type in which only dKO cells are stained for β-gal, due to the Rosa allele being included. (A,E) 8.5 dpc; others are 9.5-dpc embryos. (D,H) Magnified figures of C,G, respectively. Whole-mount β-gal staining reveals that the heart (arrows) does not contain β-gal-stained cells in the dKO/wild chimera embryo (E-H) but does so in the wild/wild chimera (A-D). Embryos shown in B and F were stained for only 4 hours. Others were stained overnight to ensure penetration of the β-gal substrate. (I-L,M-P) Histological analysis of the β-gal-stained chimeric embryos shown in C,G, respectively. The sectioning planes are indicated by white lines. (I,M) Head region. Head mesenchymal cells are composed of wild-type cells in the dKO/wild chimera. NT, neural tube; a, anterior; p, posterior. (J,K,N,O) Heart region. Most of the myocardial and endocardial cells in the dKO/wild chimera embryo are composed of wild-type cells but dKO cells contribute to the atrial appendage (arrow in O). (L,P) somitic region. Note that dermomyotome (DM) in the dKO/wild chimera embryo is composed of wild-type cells.

cranial mesoderm. Interestingly, the paraxial mesoderm was composed of both types of cells, indicating that *Mesp1*$^{-/-}$, *Mesp2*$^{-/-}$ cells can contribute to somitogenesis (Fig. 7L,P); however, a biased distribution of β-gal-positive cells was revealed after segmentation (Fig. 7P). Most dermomyotomal cells were composed of β-gal-negative wild-type cells. Furthermore, a segmental border was not clearly generated in chimeric embryos with *Mesp1*$^{-/-}$, *Mesp2*$^{-/-}$ cells compared with that in wild/wild chimeras. Because the *Mesp2*-null embryo shows a similar defect in segmentation, we are planning to conduct chimeric analysis during somitogenesis in greater detail in the future. The contribution of β-gal-positive *Mesp1*$^{-/-}$, *Mesp2*$^{-/-}$ cells to the neural tube was quite high. Other tissues, including the notochord, gut and lateral plate mesoderm, were composed of both cell types. Therefore the migration defect in the anterior cranial mesoderm and cardiac mesoderm observed in dKO embryos is deemed to be cell-autonomous, while the lack of paraxial mesoderm in dKO embryos is more likely to be a non-cell-autonomous defect.

DISCUSSION

Previous studies on *Mesp1*$^{-/-}$ embryos have revealed the requirement of MesP1 for normal heart morphogenesis (Saga, 1998; Saga et al., 1999). The primary defect leading to the abnormality is the lack of migratory activity of *Mesp1*-expressing heart precursor cells; however, the cells eventually acquired migratory activity and gave rise to an abnormal heart tube. The present study revealed that this rescue was due to the expression of another gene of the same family, *Mesp2*, which was observed in a similar pattern although at a considerably lower level, than that of *Mesp1*. In the absence of these two genes, the embryo shows failure of development of the heart, gut or somites due to the defect of the nonaxial embryonic mesoderm.

Primary defect in the dKO embryo

The major defect observed in the dKO embryo was the inability of the nonaxial mesodermal cells to migrate out from the primitive streak. Either the lack of migratory activity or the enhanced cellular adhesiveness of the cells in the primitive streak would explain this. A preliminary in vitro study on the migratory activity of mesodermal cells in the primitive streak region in 7.5-dpc embryos revealed no clear differences between wild-type and dKO embryos. Since

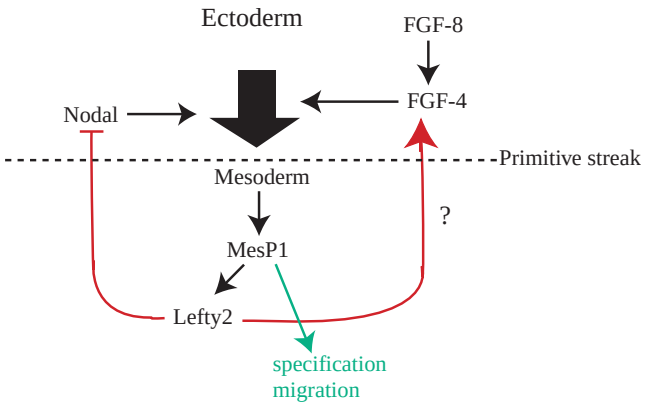

Fig. 8. Schematic representation of possible interactions of molecules between the primitive streak and the mesoderm. FGF and Nodal signaling are important for the normal function of the primitive streak (Sun et al., 1999; Conlon et al., 1994). MesP1 expressed in the mesoderm may regulate *Lefty2* positively and Lefty2 may regulate the function of the primitive streak by repressing *Nodal* expression (Meno et al., 1999) and by activating *Fgf4*. FGF-8 is known to act positively on the regulation of *Fgf4* in the primitive streak (Sun et al., 1999). Genetic activities in the mesoderm might therefore be important to maintain the normal function of the primitive streak. Arrows do not necessarily indicate direct regulation of transcription. Red lines indicate non-cell-autonomous effects, green lines, cell-autonomous effects.

at least the paraxial mesoderm in chimeric embryos was able to participate in somite formation, *Mesp1*$^{-/-}$, *Mesp2*$^{-/-}$ cells probably developed the ability to migrate once they departed from the primitive streak. Actually, the results of chimera analysis were notable. The contribution of dKO cells to the heart tissue was considerably low. This result is completely consistent with the results for the dKO embryo, which shows no migration of mesodermal cells; however, in chimeric embryos, wild-type cells migrated to the heart field and gastrulation continued, and then other mesodermal defects were rescued by wild-type cells. What happened to the dKO cells that were destined to become heart precursors but could not migrate normally? There are two possibilities. The cells might not be specified as heart precursors, or they might only lack the ability to migrate even though they were specified as the precursors. We cannot distinguish between these two unless we conduct transplantation experiments where *Mesp1*, *p2*-del cells are placed in the heart field in the wild-type embryo. If these cells were specified as the precursors, they would differentiate in the new environment, and vice versa. Alternatively, dKO cells destined to be heart precursor cells might change their developmental fate to another cell lineage such as extraembryonic, lateral or paraxial mesoderm, or axial mesendoderm. We propose that lineage analysis be performed by marking *Mesp1*-expressing cells with a cre-lox mediated recombination system in the dKO genetic background; this requires an enhancer-driven cre transgenic mice line, which is under construction.

Possible difference in the mechanism to generate extraembryonic and embryonic mesoderms

Lineage analysis of *Mesp1*-expressing cells revealed their contribution to the extraembryonic mesoderm in addition to their contribution to the heart tissues (Saga et al., 1999). The extraembryonic mesoderm of dKO embryos retained its ability to generate allantois and blood islands. The extensive blood cell differentiation contrasted with the inability of embryonic mesodermal cells to differentiate. It should be noted that the analysis of some gene-knockout mice indicated differences between the mesoderms of the extraembryonic and embryonic regions. For example, in the absence of Smad2, embryonic anterior-posterior (A-P) organization was severely affected and tissues of the embryonic germ layer were entirely absent, but a normal yolk sac and fetal blood cells were generated (Waldrip et al., 1998). It was speculated that the lack of a distinct primitive streak structure might be the reason for the entire epiblast to adopt an extraembryonic mesodermal fate. This may indicate that the extraembryonic mesoderm is generated in the absence of a normal primitive streak. Another example was the case of a mutant mouse called *eed*, in which epiblast cells ingressed through the anterior streak, but the newly formed mesoderm did not migrate anteriorly and was mislocalized to the extraembryonic compartment (Faust et al., 1998). In order to clarify whether mislocalization of the mesoderm into the extraembryonic mesoderm or into the axial mesoendoderm is responsible for the mesodermal abnormality in dKO mice, further studies using the lineage tracing experiment conducted for the *eed* embryo (Faust et al., 1998) are required.

Implication of *Mesp1* and *Mesp2* expression in heart precursor cells

Unlike other molecules directly involved in heart morphogenesis, such as *Gata-4* (Kuo et al., 1997; Molkentin et al., 1997), *Nkx2-5* (Biben and Harvey, 1997), *Hand1* (Riley et al., 1998) and *Hand2* (Srivastava et al., 1997), *Mesp1* and *Mesp2* are expressed in the nascent heart precursor cells and not during heart morphogenesis. It is therefore unlikely that MesP1 and MesP2 are involved in heart tube formation itself; rather, they may be involved in mesodermal specification. We previously reported that only the myocardium in the heart was derived from *Mesp1*-expressing cells (Saga et al., 1999). We recently found, however, that *Mesp1*-expressing cells may contain endothelial precursor cells for heart and other vascular systems, such as cranial vein, dorsal aorta and the intersomitic vascular system (our unpublished data). Therefore, MesP1 may be involved in the specification of endothelial lineages, although more detailed and careful analyses are required for definitive conclusions.

Sequential mechanism of departure from the primitive streak

Chimera analysis revealed the inability of *Mesp1*$^{-/-}$, *Mesp2*$^{-/-}$ cells to contribute to the cephalic or cardiac mesoderm. It is worth noting that the defect of *Mesp1*$^{-/-}$, *Mesp2*$^{-/-}$ cells in the chimera is strongly correlated with the expression of *Mesp1* and *Mesp2*. Both are expressed in the early ingressed groups of mesoderm destined to the extraembryonic, cranial-cardiac mesoderm, but not in the axial mesoderm or early paraxial mesoderm (expression in the paraxial mesoderm starts immediately before segmentation). Therefore, the inability of the cells to contribute to the cephalic and cardiac mesoderm must be a cell-autonomous defect. In contrast, why can the *Mesp1*$^{-/-}$, *Mesp2*$^{-/-}$ cells contribute to the paraxial and other

mesodermal derivatives in the presence of wild-type cells? We speculate that there may be some instructive mechanism to sequentially deliver the mesoderm to different lineages. Normal formation of the cranial-cardiac mesoderm may be required for normal generation and/or departure of the lateral and paraxial mesoderms, indicating that the function of the primitive streak is affected in the *Mesp1, p2*-del embryo. Regarding the function of the primitive streak, it is noted that a similar phenotype of mesodermal defect is reported in the *Fgf8*-null embryo, the cause of which is suspected to be the lack of *Fgf4* expression. Therefore, it is likely that MesP1 and MesP2 function downstream of FGF signaling. Although the expression of *Fgf8* was not affected in the *Mesp1, p2*-del embryo, no *Fgf4* expression was observed, which suggests that MesP1 and MesP2 are required for the maintenance of *Fgf4* expression in the primitive streak. Therefore, we suggest the existence of some reciprocal interaction between the primitive streak and the mesoderm to maintain the function of the primitive streak for constant epithelial-to-mesenchymal transition to deliver all mesodermal layers (Fig. 8). We speculate that *Lefty2* may be a possible downstream target of MesP1and MesP2, and the gene product is a candidate for the signaling molecule responsible for modulating the genetic activity in the primitive streak. Actually, the *Lefty2*-null embryo has an expanded primitive streak and forms excess mesoderm by allowing the overexpression of Nodal signaling in the primitive streak. The effect is shown to be mediated by a feedback loop wherein Nodal signals induce their antagonist Lefty2 to restrict Nodal signaling during gastrulation (Meno et al., 1999). Therefore, MesP1 and MesP2 may affect the genetic activities in the primitive streak (e.g. *Fgf4* or *Nodal* expression) by regulating *Lefty2* expression. In the chimera embryo, the function of primitive streak must be maintained by this type of non-cell-autonomous signaling by the wild-type cells. However, *Mesp1*$^{-/-}$, *Mesp2*$^{-/-}$ cells could not migrate and contribute to the heart tissues, indicating that a cell-autonomous function of MesP1 and MesP2 is required for the further specification and/or migration of cardiac mesodermal cells.

The axial mesoderm, in which neither *Mesp1* nor *Mesp2* was expressed as in the case of the paraxial mesoderm, was, however, generated in the *Mesp1, p2*-del embryo by at least at 7.5 dpc, although it regressed during the later stage of development. This observation suggests that a separate mechanism may be operating for the generation of the axial mesoderm.

Neural patterning in the *Mesp1, p2*-del embryo

Another notable finding in the *Mesp1, p2*-del phenotype is the biased neural patterning. A headfold-like structure generated in the *Mesp1, p2*-del embryo exhibited only anterior neural character and no posterior properties. Recent extensive studies revealed that several molecules, such as *Hesx1, Hex1, Cer1, Otx2* and *Lim1,* are involved in the induction or maintenance of the anterior head properties in vertebrates (Beddington and Robertson, 1999). These molecules are initially expressed in the visceral endoderm and are replaced with the anterior mesendoderm, while the posterior mesendoderm may antagonize the anterior-inducing activity to restrict the anterior region and secure posterior neural region. Actually, in the *Mesp1, p2*-del embryo, *Cerl* is strongly expressed in the endoderm and the expression is not restricted to the anterior region but is rather widespread throughout the entire embryo. A similar neuronal phenotype was observed in the *Fgf8*-null embryo. This was explained by the lack of proximal displacement of the anterior visceral endoderm, due to failure of definitive endoderm cells to migrate rostrally. Actually, molecular markers of mesendodermal cells, *Hnf-3b, Hnf3a, Gsc* or *Shh*, were expressed only in the posterior region and never extended anteriorly in the *Fgf8*-null embryo (Sun et al., 1999). In the *Mesp1, p2*-del embryo, however, strong *Hnf-3b* expression was observed throughout the endoderm, including the anterior region. Because *Hnf-3b* is expressed in both visceral and definitive endoderms, *Hnf-3b* expressing cells in the *Mesp1, p2*-del embryo should represent either one or both. In contrast, *Hnf3a*, which is only expressed in the definitive endoderm and its precursors, and *Gsc*, which is a marker of the anteriormost mesendoderm, the prechodal plate, were observed in the posterior region and not in the anterior region of the *Mesp1, p2*-del embryo. Thus, it is likely that *Hnf-3b* expression in the visceral endoderm of *Mesp1, p2*-del embryo is retained by the lack of displacement with the definitive endoderm, similar to the case of *Fgf8*-null embryo. Genetic activity in the visceral endoderm appeared to be maintained longer and stronger in the case of the *Mesp1, p2*-del embryo than in that of the *Fgf8*-null embryo. The lack of a posterior neural marker would be caused by the lack of a posterior mesendoderm, being also due to the failure of displacement of the definitive endoderm. The signals antagonizing anterior-inducing signals must be lacking in both *Mesp1, p2*-del and *Fgf8*-null embryos. The determination of posteriorizing signals derived from either the definitive endoderm or the mesoderm would be important for further understanding of the regulation of neural patterning.

We are grateful to the following researchers for providing reagents: Alvert F. Candia (*Mox1* cDNA), Bernhard G. Herrmann (*Brachyury* cDNA), Hiroshi Sasaki (*Hnf3a* and *Hnf-3b* cDNA), Shinichi Aizawa (*Otx2* cDNA), Hiroshi Hamada (*Lefty2* cDNA), Masanori Taira *(Lim1* cDNA), Rosa Beddington (*Hex* cDNA,) Gen Yamada (*Goosecoid* cDNA), Gail Martin (*Fgf4* cDNA), Peter Gruss (*Six3* cDNA), Eddy M. De Robertis (*Cereberus-like-1* cDNA) and Peter W. Laird (*puromycin* cDNA). We also thank Hiroshi Uejima for FISH analysis and Wakako Murai and Mariko Ikumi for general technical assistance. This work was supported in part by grants from the Ministry of Education, Science, Sports and Culture, Japan and by special coordination funds for promoting science and technology from the Science and Technology Agency in Japan.

REFERENCES

Ang, S. L., Conlon, R. A., Jin, O. and Rossant, J. (1994). Positive and negative signals from mesoderm regulate the expression of mouse Otx2 in ectoderm explants. *Development* **120**, 2979-2989.

Beddington, R. S. and Robertson, E. J. (1999). Axis development and early asymmetry in mammals. *Cell* **96**,195-209.

Biben, C. and Harvey, R. P. (1997). Homeodomain factor Nkx2.5 controls left/right asymmetric expression of bHLH gene *eHand* during murine heart development. *Genes Dev*. **11**, 1357-1369.

Blum, M., Gaunt, S. J., Cho, K. W., Steinbeisser, H., Blumberg, B., Bittner, D. and De Robertis, E. M. (1992). Gastrulation in the mouse: the role of the homeobox gene *goosecoid. Cell* **69**, 1097-1106.

Candia, A. F., Hu, J., Crosby, J., Lalley, P. A., Noden, D., Nadeau, J. H. and Wright, C. V. E. (1992). *Mox-1* and *Mox-2* define a novel homeobox gene subfamily and are differentially expressed during early mesodermal patterning in mouse embryos. *Development* **116**, 1123-1136.

Chapman, D. L., Garvey, N., Hancock, S., Alexiou, M., Agulnik, S. I., Gibson-Brown, J. J., Cebra-Thomas, J., Bollag, R. J., Silver, L. M. and Papaioannou, V. E. (1996). Expression of the T-box family genes, *Tbx1-Tbx5*, during early mouse development. *Dev. Dyn.* **206**, 379-390.

Clements, D., Taylor, H. C., Herrmann, B. G. and Stott, D. (1996). Distinct regulatory control of the *Brachyury* gene in axial and non-axial mesoderm suggests separation of mesoderm lineages early in mouse gastrulation. *Mech. Dev.* **56**,139-49.

Conlon, F. L., Lyons, K. M., Takaesu, N., Barth, K. S., Kispert, A., Herrmann, B. and Robertson, E. J. (1994). A primary requirement for nodal in the formation and maintenance of the primitive streak in the mouse. *Development* **120,** 1919-1928.

Crossley, P. H. and Martin, G. R. (1995). The mouse Fgf8 gene encodes a family of polypeptides and is expressed in regions that direct outgrowth and patterning in the developing embryo. *Development* **121**,439-451.

DeRuiter, M. C., Poelmann, R. E., VanderPlas-de Vries, I., Mentink, M. M. and Gittenberger-de Groot, A. C. (1992). The development of the myocardium and endocardium in mouse embryos. Fusion of two heart tubes? *Anat. Embryol. (Berl.)*, **185**, 461-473.

Ding, J., Yang, L., Yan, Y. T., Chen, A., Desai, N., Wynshaw-Boris, A. and Shen, M. M. (1998). Cripto is required for correct orientation of the anterior-posterior axis in the mouse embryo. *Nature* **395**, 702-707.

Faust, C., Schumacher, A., Holdener, B. and Magnuson T. (1995). The eed mutation disrupts anterior mesoderm production in mice. *Development* **121**, 273-285.

Faust, C., Lawson, K. A., Schork, N. J., Thiel, B. and Magnuson, T. (1998). The Polycomb-group gene *eed* is required for normal morphogenetic movements during gastrulation in the mouse embryo. *Development* **125**, 4495-4506.

Herrmann, B. G., Labeit, S., Poustka, A., King, T. R. and Lehrach, H. (1990). Cloning of the *T* gene required in mesoderm formation in the mouse. *Nature* **343**, 617-622.

Holdener, B. C., Faust, C., Rosenthal, N. S. and Magnuson, T. (1994). msd is required for mesoderm induction in mice. *Development* **120**, 1335-1346.

Kuo, C. T., Morrisey, E. E., Anandappa, R., Sigrist, K., Lu, M. M., Parmacek, M. S., Soudais, C. and Leiden, J. M. (1997). GATA4 transcription factor is required for ventral morphogenesis and heart tube formation. *Genes Dev*. **11**, 1048-1060.

Lawson, K. A. and Pedersen, R. A. (1992). Clonal analysis of cell fate during gastrulation and early neurulation in the mouse. In postimplantation development in the mouse. *Ciba Found. Symp.* **165**, 3-26.

Lawson, K. A., Meneses, J. J. and Pedersen, R. A. (1991). Clonal analysis of epiblast fate during germ layer formation in the mouse embryo. *Development* **113**, 891-911.

Matsuo, I., Kuratani, S., Kimura, C., Takeda, N., and Aizawa, S. (1995). Mouse Otx2 functions in the formation and patterning of rostral head. *Genes Dev*. **9**, 2646-2658.

Meno, C., Gritsman, K., Ohishi, S., Ohfuji, Y., Heckscher, E., Mochida, K., Shimono, A., Kondoh, H., Talbot, W. S., Robertson, E. J., Schier, A. F. and Hamada, H. (1999). Mouse Lefty2 and zebrafish antivin are feedback inhibitors of nodal signaling during vertebrate gastrulation. *Mol. Cell* **4**, 287-298.

Molkentin, J. D., Lin, Q., Duncan, S. A. and Olson, E. N. (1997). Requirement of the transcription factor GATA4 for heart tube formation and ventral morphogenesis. *Genes Dev*. **11**, 1061-1072.

Oliver, G., Mailhos, A., Wehr, R., Copeland, N. G., Jenkins, N. A. and Gruss, P. (1995). *Six3*, a murine homologue of the sine oculis gene, demarcates the most anterior border of the developing neural plate and is expressed during eye development. *Development* **121**, 4045-4055.

Parameswaran, M. and Tam, P. (1995). Regionalisation of cell fate and morphogenetic movement of the mesoderm during mouse gastrulation. *Dev. Genet.* **17**, 16-28.

Perea-Gomez, A., Shawlot, W., Sasaki, H., Behringer, R. R. and Ang, S. (1999). HNF3beta and Lim1 interact in the visceral endoderm to regulate primitive streak formation and anterior-posterior polarity in the mouse embryo. *Development* **126**, 4499-4511.

Riley, P., Anson-Cartwright, L. and Cross, J. C. (1998). The Hand1 bHLH transcription factor is essential for placentation and cardiac morphogenesis. *Nat. Genet.* **18**, 271-275.

Saga, Y. (1998). Genetic rescue of segmentation defect in MesP2-deficient mice by MesP1 gene replacement. *Mech. Dev*. **75**, 53-66.

Saga, Y., Hata, N., Kobayashi, S., Magnuson, T., Seldin, M. and Taketo, M. M. (1996). MesP1: A novel basic helix-loop-helix protein expressed in the nascent mesodermal cells during mouse gastrulation. *Development* **122**, 2769-2778.

Saga, Y., Hata, N., Koseki, H. and Taketo, M. M. (1997). *Mesp2*: a novel mouse gene expressed in the presegmented mesoderm and essential for segmentation initiation. *Genes Dev*. **11**, 1827-1839.

Saga, Y., Miyagawa-Tomita, S., Takagi, A., Kitajima S. Miyazaki, J. and Inoue, T. (1999). MesP1 is expressed in the heart precursor cells and required for the formation of a single heart tube. *Development* **126**, 3437-3447.

Saga, Y., Yagi, T., Ikawa, Y., Sakakura, T. and Aizawa, S. (1992). Mice develop normally without tenascin. *Genes Dev.* **6**, 1821-1831.

Sasaki, H. and Hogan, B. L. (1993). Differential expression of multiple fork head related genes during gastrulation and axial pattern formation in the mouse embryo. *Development* **118**, 47-59.

Shalaby, F., Ho, J., Stanford, W. L., Fischer, K. D., Schuh, A. C., Schwartz, L., Bernstein, A. and Rossant, J. (1997). A requirement for Flk1 in primitive and definitive hematopoiesis and vasculogenesis. *Cell* **89**, 981-990.

Srivastava, D., Thomas, T., Lin, Q., Kirby, M. L., Brown, D. and Olson, E. N. (1997). Regulation of cardiac mesodermal and neural crest development by the bHLH transcription factor, dHAND. *Nat. Genet.* **16**, 154-160.

Sun, X., Meyers, E. N., Lewandoski, M. and Martin, G. R. (1999). Targeted disruption of *Fgf8* causes failure of cell migration in the gastrulating mouse embryo. *Genes Dev.* **13**, 1834-1846.

Tam, P. P. L. and Behringer, R. R. (1997). Mouse gastrulation: the formation of a mammalian body plan. *Mech. Dev*. **68**, 3-25.

Tam, P. P. L., Parameswaran, M., Kinder, S. J. and Weinberger, R. P. (1997). The allocation of epiblast cells to the embryonic heart and other mesodermal lineages: the role of ingression and tissue movement during gastrulation. *Development* **124**, 1631-1642.

Thomas, P. Q., Brown, A. and Beddington, R. S. (1998). *Hex:* a homeobox gene revealing peri-implantation asymmetry in the mouse embryo and an early transient marker of endothelial cell precursors. *Development* **125**, 85-94.

Waldrip, W. R., Bikoff, E. K., Hoodless, P. A., Wrana, J. L. and Robertson, E. J. (1998). Smad2 signaling in extraembryonic tissues determines anterior-posterior polarity of the early mouse embryo. *Cell* **92**, 797-808.

Wassarman, K. M., Lewandoski, M., Campbell, K., Joyner, A. L., Rubenstein, J. L., Martinez, S. and Martin, G. R. (1997). Specification of the anterior hindbrain and establishment of a normal mid/hindbrain organizer is dependent on *Gbx2* gene function. *Development* **124**, 2923-2934.

Watanabe, S., Kai, N., Yasuda, M., Kohmura, N., Sanbo, M., Mishina, M. and Yagi, T. (1995). Stable production of mutant mice from double gene converted ES cells with puromycin and neomycin. *Biochem. Biophys. Res. Commun.* **213**, 130-137.

Yagi, T., Tokunaga, T., Furuta, Y., Nada, S., Yoshida, M., Tsukada, T., Saga, Y., Takeda, N., Ikawa, Y. and Aizawa, S. (1993). A novel ES cell line, TT2, with high germline-differentiating potency. *Anal. Biochem.* **214**, 70-76.

Yamaguchi, T. P., Harpal, K., Henkemeyer, M. and Rossant J. (1994). *fgfr-1* is required for embryonic growth and mesodermal patterning during mouse gastrulation. *Genes Dev*. **8**, 3032-3044.

Zambrowicz, B. P., Imamoto, A., Fiering, S., Herzenberg, L. A., Kerr, W. G. and Soriano, P. (1997). Disruption of overlapping transcripts in the ROSA beta geo 26 gene trap strain leads to widespread expression of beta-galactosidase in mouse embryos and hematopoietic cells. *Proc. Natl. Acad. Sci. USA* **94**, 3789-3794.

Zhou, X., Sasaki, H., Lowe, L., Hogan, B. L. and Kuehn, M. R. (1993). *Nodal* is a novel TGF-beta-like gene expressed in the mouse node during gastrulation. *Nature* **361**, 543-547.